Iuliacumite: A Novel Chemical Short-Range Order in a Two-Dimensional Wurtzite Single Monolayer InAs$_{1-x}$Sb$_x$ Shell on InAs Nanowires

M. Schnedler,[*,†] T. Xu,[‡,¶] I. Lefebvre,[‡] J.-P. Nys,[‡] S. R. Plissard,[‡,§] M. Berthe,[‡] H. Eisele,[‖] R. E. Dunin-Borkowski,[†] Ph. Ebert,[†] and B. Grandidier[*,‡]

[†]Peter Grünberg Institut, Forschungszentrum Jülich GmbH, 52425 Jülich, Germany

[‡]Université Lille, CNRS, Centrale Lille, ISEN, Université Valenciennes, UMR 8520 - IEMN, F-59000 Lille, France

[¶]Key Laboratory of Advanced Display and System Application, Shanghai University, 149 Yanchang Road, Shanghai 200072, People's Republic of China

[§]CNRS-Laboratoire d'Analyse et d'Architecture des Systèmes (LAAS), Université de Toulouse, 7 Avenue du Colonel Roche, 31400 Toulouse, France

[‖]Institut für Festkörperphysik, Technische Universität Berlin, Hardenbergstr. 36, 10623 Berlin, Germany

ABSTRACT: A chemical short-range order is found in single monolayer InAs$_{1-x}$Sb$_x$ shells, which inherit a wurtzite structure from the underlying InAs nanowire, instead of crystallizing in the energetically preferred zincblende structure. The chemical order is characterized by an anticorrelation ordering vector in the $\langle 11\bar{2}0 \rangle$ direction and arises from strong Sb−Sb repulsive interactions along the atomic chains in the $\langle 11\bar{2}0 \rangle$ direction.
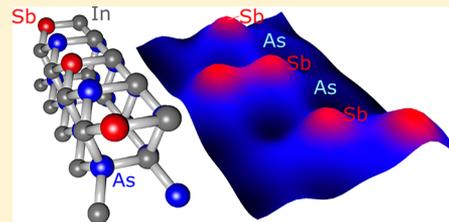
KEYWORDS: *Chemical ordering, single monolayer, wurtzite, In(As,Sb), nanowire shell*

The reduced dimensionality of semiconductor nanowires (NWs) offers the unique opportunity to grow materials with crystal structures that are otherwise unstable. One of the most prominent examples is the growth of wurtzite (WZ) structure InAs NWs,[1] although stable InAs bulk material prefers the zincblende (ZB) structure. In contrast, other III−V materials, notably InAs$_{1-x}$Sb$_x$, prefer to keep their ZB bulk structure even in NWs or nanostructures with reduced dimensionality.[2,3] However, lateral overgrowth of these ternary III−V semiconductor alloys on sidewall facets of WZ structure III−V nanowires offers the prospect to nevertheless obtain reliably a WZ structure shell, despite being unstable. Thereby new polytype structures of ternary III−V semiconductor alloys can be achieved, offering additional degrees of freedom for adjusting the band structure in, for example, core−shell nanowires.

In addition to controlling the polytype structure, controlling ordering of the different chemical species in ternary III−V semiconductor alloys offers further means to tune the electrical properties. This has been amply demonstrated for ZB structure III−V semiconductors, where a variety of different chemical ordering structures were identified (i.e., chalcopyrite, CuPt, CuAu, famatinite, triple period, and lazarevicite).[4−9] In contrast, rather little is known about chemical ordering in WZ structure III−V semiconductors. Thus, far most reports on chemical ordering refer to *c* axis ordering and superlattices in WZ structure group III-nitride semiconductors.[10−17] Only during growth on pyramidal pits ordering along the pit's

semipolar growth facets was observed.[18] In contrast to the limited experimentally observed ordering structures in WZ materials, theory predicts a large variety of possible ordered WZ structures, with ordering vectors not only in *c* direction,[19,20] but without experimental verification yet.

Furthermore, thus far chemical ordering in III−V semiconductor alloys was experimentally identified in (quasi) three-dimensional materials, that is, bulk or extended nanowire bulk-like sections. However, lateral overgrowth on NW sidewall facets offers the possibility to obtain monolayer thin two-dimensional ternary III−V semiconductor sheets. At present, it is unclear if any chemical ordering is forming in such two-dimensional WZ-structure III−V semiconductors or in general in emerging groups of two-dimensional ternary semiconductor materials.[21−23]

Therefore, we designed a two-dimensional single monolayer InAs$_{1-x}$Sb$_x$ WZ structure shell on sidewall facets of InAs nanowires and investigated its chemical ordering using atomically resolved scanning tunneling microscopy (STM). We identify the existence of a short-range chemical ordering in this WZ structure single monolayer shell. The new type of ordering in a two-dimensional sheet, called iuliacumite, is characterized by an antiordering vector in $\langle 11\bar{2}0 \rangle$ direction. The ordering is driven by a strong repulsive interaction of

neighboring Sb atoms along the $\langle 11\bar{2}0\rangle$-oriented atomic chains on the m plane sidewall facets.

In order to fabricate two-dimensional single WZ structure III−V semiconductor monolayers, [0001] oriented WZ InAs NW segments were overgrown *in situ* by $InAs_{1-x}Sb_x$ at 410 °C using gas source molecular beam epitaxy. After growth, a thin capping layer of As was deposited onto the nanowire surfaces to prevent oxidation during transport through air into the analysis system. There, the nanowires were heated under UHV conditions to remove the capping layer. After cleaning, the NWs were cleaved off and transferred to a freshly cleaned Si(111) surface, to investigate their sidewalls *in situ* by STM.[2,9]

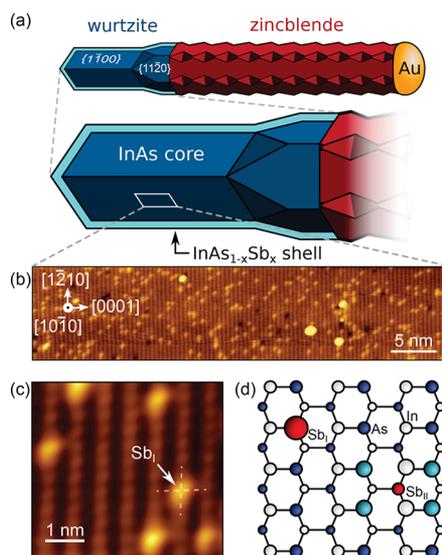Figure 1a illustrates schematically the structure of the investigated NWs, with the WZ structure InAs core in blue and

Figure 1. (a) Schematic of the $[\overline{111}]$ grown WZ structure InAs core in blue and the axially grown $InAs_{1-x}Sb_x$ ZB structure segment in red. During axial growth an additional lateral overgrowth on the sidewall facets of the InAs core by WZ structure $InAs_{1-x}Sb_x$ occurs (light blue). (b) Atomically resolved constant-current STM image of the overgrown sidewall surface measured at 77 K, using a sample voltage of −3 V and a tunnel current of 10 pA. Under these tunneling conditions, the filled dangling bond states above the surface anions are imaged. (c) Magnified STM image showing the atomic rows in detail. The bright atomically localized contrast features arise from substitutional Sb atoms on As sites. (d) Atomic ball model of Sb atoms in different subsurface layers (same orientation as the STM image), illustrating different symmetries of the Sb contrast on the surface: Sb atoms incorporated on As sites in the surface layer (denoted as Sb_I) can be observed as protrusions centered on top of an anion sublattice site in the STM image. In contrast, Sb atoms incorporated in the second atomic layer (Sb_{II}) can be anticipated to give rise to an outward relaxation of four surface As atoms (light blue balls) and thus a protrusion centered between the atomic chains. Since such contrast features are never observed, the second atomic layer is free of Sb, indicating the presence of only a single monolayer thick $InAs_{1-x}Sb_x$ shell.

the axially grown $InAs_{1-x}Sb_x$ ZB structure segment in red. As illustrated below, during axial growth also a lateral overgrowth of WZ structure $InAs_{1-x}Sb_x$ on the InAs NW sidewall facets occurs (light blue). Here we focus on these overgrown $(10\bar{1}0)$ sidewall facets. Figure 1b illustrates an atomically resolved filled-state STM image of a sidewall facet acquired at negative sample bias. Under these conditions, the filled dangling bonds

above every group V atom are imaged. First of all, the symmetry and lattice constants demonstrate that the overgrown layer kept the WZ structure of the InAs core.[24] Second, the surface exhibits a high density of atomically sized protrusions (see magnification in Figure 1c), arising from the presence of substitutional Sb atoms on As lattice positions. The contrast arises primarily from the outward relaxation induced by the Sb atoms with larger atomic radii as compared to the As atoms of the host lattice, in analogy to Sb atoms in ZB structure (110) III−V surfaces.[25]

At closer look, all protrusions exhibit identical symmetries and intensities, centered exactly on top of a surface As sublattice position. Considering the crystal symmetry, substitutional Sb atoms in different layers in and below the surface exhibit different symmetries of the Sb contrast on the surface (Figure 1d). Protrusions centered on top of the surface As sublattice sites are compatible with Sb atoms incorporated on As sites in the surface layer, as schematically illustrated in the atomic model for the case labeled Sb_I in Figure 1d. In contrast, a Sb atom in the second layer (Sb_{II}) is centered between four surface As atoms, which can be anticipated to relax outward due to the larger Sb atom (as indicated by the larger size of the slightly lighter blue balls representing the neighboring As atoms in Figure 1d), in analogy to impurities in ZB structure (110) III−V semiconductor surfaces.[26−29] Hence, an Sb atom in the second layer would create a bright contrast with a mirror symmetry between the atomic rows along the c direction. Such a contrast is never observed, even not in local areas free of surface Sb atoms. Hence, Sb is not present in the second layer, indicating that the laterally overgrown $InAs_{1-x}Sb_x$ shell is a two-dimensional sheet, only a single monolayer thick. A count of the Sb protrusions yields concentrations ranging between 6.3% and 9.8% for our NWs.

This raises the question why the sidewall overgrowth by WZ structure $InAs_{1-x}Sb_x$ is limited to only one monolayer at our growth conditions. This limitation implies that nuclei of islands on top of the single monolayer shell are unstable and hence Sb atoms prefer incorporation in the axially grown upper ZB structure $InAs_{1-x}Sb_x$ section. This is conceivable, since $InAs_{1-x}Sb_x$ prefers the ZB structure even at very small Sb concentrations. However, overgrowth on sidewalls facets of WZ structure InAs NWs forces $InAs_{1-x}Sb_x$ to crystallize in the WZ structure of the InAs core. In addition, an inward diffusion of Sb is energetically prohibited,[30] and Sb as a surfactant has the tendency to float,[31] both leading to incorporation only in the surface layer and hence stabilizing the single monolayer $InAs_{1-x}Sb_x$ WZ structure shell.

The above discovery of a single monolayer shell raises the question whether (short-range) chemical ordering can emerge and how it might look like in such two-dimensional WZ structure $InAs_{1-x}Sb_x$ monolayer sheets. For identifying a possible short-range order, we mapped the spatial distribution of the group V elements in the $InAs_{1-x}Sb_x$ monolayer shell with atomic resolution. This chemical map is then used for an in-depth analysis of the spatial correlation of the Sb distribution. Figure 2a illustrates the two-dimensional pair-correlation function (PCF), $c(x, y)$, for Sb atoms. Values close to one represent statistically expected Sb pair distributions without interactions. Hence the data shows that at larger distances no interactions are present. However, for nearest neighbor Sb pairs along the a direction, the PCF exhibits values much smaller than 1, indicating a low probability of occurrence (for quantitative comparability, see Figure 2b). In
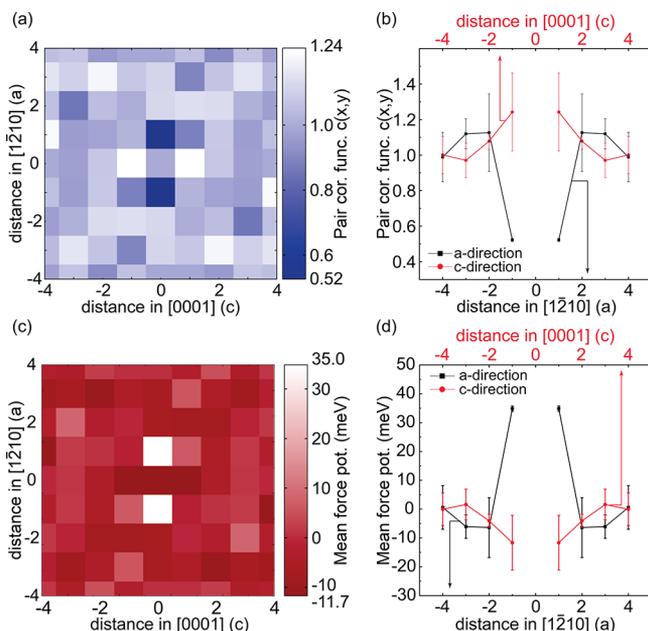
Figure 2. (a) Heat map of the two-dimensional Sb pair correlation function $c(x, y)$ within the WZ structure InAs$_{1-x}$Sb$_x$ single monolayer sheet. Values above (below) 1 indicate a higher (lower) than statistically expected occurrence of Sb pairs without interaction (scale on the right). (b) Cross sections of the PCF $c(x, y)$ along (a direction) and across (c direction) the atomic rows. For nearest neighbor Sb pairs along the a direction the PCF exhibits values much smaller than 1, indicating a strong repulsion. (c) Heat map of the two-dimensional mean force potential $W(x, y) = -kT \ln[c(x, y)]$ derived from the experimentally measured PCF. (d) Cross sections of the mean force potential in a and c directions. Nearest neighbor Sb pairs in the a direction exhibit a repulsive interaction energy of about +35 meV, whereas in the c direction a weak attractive interaction energy of about −12 meV occurs.

contrast, nearest neighbor Sb pairs in c direction, that is, across the atomic chains, exhibit PCF values slightly larger than 1, indicating slightly more frequent occurrences than statistically expected. The results emphasize that a strong anticorrelation in $[1\bar{2}10]$ and only a weak correlation in $[0001]$ direction define the chemical short-range order. This yields an antiordering vector $\underline{v}_{AO} = \frac{2}{3}a[1\bar{2}10]$ and an ordering vector $\underline{v}_O = c[0001]$

In order to investigate possible Sb concentration effects, we extracted the pair correlation values for nearest neighbor Sb pairs in the a direction for local surface areas with low (6.3%) and with higher (9.8%) Sb concentration. We obtained values of 0.512 and 0.528 for 6.3% and 9.8% Sb, respectively. Hence, this indicates that the anticorrelation ordering in the a direction is concentration independent.

For a further understanding of the underlying physical mechanisms driving the ordering, we derive the so-called mean force potential, $W(x, y) = -kT \ln[c(x, y)]$,[32] which is a first approximation of the pair interaction potential in the low density limit. Here, k is the Boltzmann constant, and T is the freeze-in temperature, below which no diffusion or site changes within the InAs$_{1-x}$Sb$_x$ monolayer occur anymore. An upper limit for T is assumed to be 623 K, the temperature used for evaporation of the As cap. The resulting mean force potential, shown in Figure 2c,d, reveals a strong Sb−Sb repulsion with a repulsive energy of about 35 meV in the a direction and an Sb−Sb attraction with an attractive energy of about 12 meV in

the c direction. Hence, the energy difference between both configurations is approximately 47 ± 11 meV.

This value is compared to density function theory computations of the total energy difference of an InAs($10\bar{1}0$) surface layer that exhibits nearest neighbor Sb−Sb pairs in either c or a direction. The calculations were carried out using the Vienna ab initio simulation program (version 5.2.11).[33] All electron projector augmented wave (PAW) pseudopotentials were taken[34] using the Ceperley and Alder approximation,[35] parametrized by Perdew and Zunger for exchange and correlation energies (i.e., the Sb, As, In, H1.25 and H.75 PAW potentials).[9] We used a kinetic energy cutoff of 312.5 eV. The calculations were performed for ($10\bar{1}0$) oriented supercells with different sizes of 4 × 4, 4 × 5, and 5 × 5 and thicknesses of 8 as well as 10 monolayers (H terminated on back side). The supercells were optimized until forces on atoms were smaller than 0.9 meV/Å. The calculations yield similar total energies for all supercells. The average energy difference between Sb−Sb nearest neighbors in the c and a direction is found to be 24 meV, with pairs in the c direction being lower in energy. Note, nearest neighbor Sb−Sb pairs along the zigzag chains on the cubic ZB (110) surfaces exhibit a very similar bonding structure and indeed a very similar interaction energy of 33 meV was calculated and experimentally verified.[9]

The calculated and experimental energy differences for pairs in c and a directions are on the same order; especially the energy for pairs in the c direction is lower than for those in the a direction. This can be understood by considering the incorporation of Sb atoms with larger atomic radii in the WZ crystal structure: In the c direction, the bonding structure is less rigid, and nearest neighbor Sb atoms on the surface are in fact second nearest neighbor group V atoms (neglecting the interbonded group III atoms), since only every second (0001) plane is visible in filled (or empty) state STM images (see schematic in Figure 1d). In contrast, for Sb pairs along the a direction the Sb atoms are much closer since they are nearest neighbor group V atoms separated only by one group III atom. This enhances strain for such Sb pairs, in analogy with similarly bonded Sb pairs along the zigzag chain on ZB structure (110) surfaces.[9]

At this stage, we compare quantitatively the measured and calculated energy differences between the Sb pairs in the c and a direction. The experimental value is somewhat larger than the calculated one. However, the experimental determination suffers from the uncertainty of the freeze-in temperature and from many body effect in the pair interactions. First, the freeze-in temperature is an upper limit and thus lower in reality. Hence, the measured energy difference is likely overestimated and can be anticipated to be lower by roughly 10−15 meV. Second, at the given Sb concentrations and interaction ranges, many body effects in Sb−Sb interaction can be anticipated to be present, since the ratio between concentration and interaction length is in analogy to that of dopant atoms in GaAs, where many body effects were shown to affect pair correlation functions.[36] Hence, the mean force potential cannot be assumed to be equal to the pair interaction energy anymore and thus many body effects affect the measured energy difference. Although a quantitative agreement of the measured and calculated pair interaction energies is difficult to reach due to the mentioned effects, both the experimental and theoretical results lead to the same physical conclusion, that is,

the presence of a novel short-range order in a two-dimensional WZ structure $InAs_{1-x}Sb_x$ monolayer shell.

The experimental results yielded a very pronounced anticorrelation short-range ordering along the *a* direction, which is found to be independent of the Sb concentration. On this basis, we derive an *idealized* long-range chemical ordering structure of the monolayer shell on the InAs sidewall facet, reached at the compositional limit of $InAs_{0.5}Sb_{0.5}$ in the top plane (lower planes are pure InAs). This idealized ordering structure is given schematically in side and top view in Figure 3a,b, respectively. It consists of alternating Sb and As atoms in
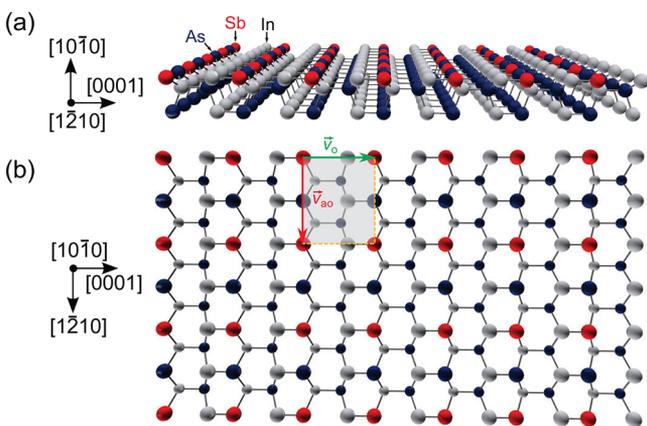

Figure 3. Perspective view of a ball model of the idealized, long-range, chemical ordering of the two-dimensional monolayer shell on the InAs sidewall facet, based on the ordering and antiordering vectors extracted from pair correlation function. (a) Side and (b) top view with surface unit cell (gray shaded area) and ordering as well as antiordering vectors shown as green and red arrows, respectively.

the atomic rows along the *a* direction. This is the result of the short-range antiordering vector $\underline{v}_{AO}$ along the *a* direction. Along the *m* direction, we chose the periodic continuation of these one-dimensional ordered rows. However, since the ordering in *m* direction is weak, it is also conceivable that a certain fraction of the alternating Sb and As occupied atomic rows along the *a* direction may be phase shifted (by one lattice constant). Therefore, the ordering should be considered as a one-dimensional ordering in a two-dimensional single monolayer shell. This one-dimensional chemical order structure is named iuliacumite, derived from the Latin name of the city of Jülich.

In conclusion, we identified a novel short-range chemical ordering type in single monolayer $InAs_{1-x}Sb_x$ wurtzite structure shells on *m* plane sidewall facets of InAs nanowires by direct atomically resolved elemental mapping using scanning tunneling microscopy. The ordering is driven by strong Sb−Sb repulsions along the atomic chains in the *a* direction, giving rise to an anticorrelation ordering in nonpolar directions, deviating from ordering in bulk WZ structure material observed thus far. This highlights the importance of spatial confinement for the formation of novel chemical ordering structures in III−V semiconductor alloys. Such chemical ordering effects in atomically thin structures may offer new degrees of adjusting and controlling the electronic properties in systems with reduced dimensions. Finally, it is also conceivable that the here observed ordering in a two-dimensional single monolayer may lead through exotic growth schemes to new types of bulk ordering.

AUTHOR INFORMATION

Corresponding Authors
*E-mail: m.schnedler@fz-juelich.de.
*E-mail: bruno.grandidier@isen.iemn.univ-lille1.fr.

ORCID
Ph. Ebert: 0000-0002-2022-2378

Notes
The authors declare no competing financial interest.

REFERENCES

(1) Caroff, P.; Wagner, J. B.; Dick, K. A.; Nilsson, H. A.; Jeppsson, M.; Deppert, K.; Samuelson, L.; Wallenberg, L. R.; Wernersson, L. *Small* **2008**, *4*, 878−882.

(2) Xu, T.; Dick, K. A.; Plissard, S.; Nguyen, T. H.; Makoudi, Y.; Berthe, M.; Nys, J.-P.; Wallart, X.; Grandidier, B.; Caroff, P. *Nanotechnology* **2012**, *23*, No. 095702.

(3) Gorji Ghalamestani, S.; Lehmann, S.; Dick, K. A. *Nanoscale* **2016**, *8*, 2778−2786.

(4) Wei, S.-H.; Zunger, A. *Phys. Rev. B: Condens. Matter Mater. Phys.* **1989**, *39*, 3279−3304.

(5) Zunger, A.; Mahajan, S. In *Handbook on Semiconductors: Materials, Properties and Preparation*; Mahajan, S., Ed.; North-Holland, 1994; Vol. *3B*, pp 1399−1514.

(6) Gomyo, A.; Makita, K.; Hino, I.; Suzuki, T. *Phys. Rev. Lett.* **1994**, *72*, 673−676.

(7) Mascarenhas, A. *Spontaneous Ordering in Semiconductor Alloys*; Kluwer Academic/Plenum Publishers: New York, 2002.

(8) Wu, M.; Luna, E.; Puustinen, J.; Guina, M.; Trampert, A. *Appl. Phys. Lett.* **2014**, *105*, No. 041602.

(9) Schnedler, M.; Lefebvre, I.; Xu, T.; Portz, V.; Patriarche, G.; Nys, J.-P.; Plissard, S. R.; Caroff, P.; Berthe, M.; Eisele, H.; Dunin-Borkowski, R. E.; Ebert, Ph.; Grandidier, B. *Phys. Rev. B: Condens. Matter Mater. Phys.* **2016**, *94*, 195306.

(10) Albrecht, M.; Lymperakis, L.; Neugebauer, J.; Northrup, J. E.; Kirste, L.; Leroux, M.; Grzegory, I.; Porowski, S.; Strunk, H. P. *Phys. Rev. B: Condens. Matter Mater. Phys.* **2005**, *71*, No. 035314.

(11) Korakakis, D.; Ludwig, K. F.; Moustakas, T. D. *Appl. Phys. Lett.* **1997**, *71*, 72−74.

(12) Iliopoulos, E.; Ludwig, K. F.; Moustakas, T. D. *J. Phys. Chem. Solids* **2003**, *64*, 1525−1532.

(13) Woicik, J. C.; Ludwig, K. F.; Moustakas, T. D. *Appl. Phys. Lett.* **2012**, *100*, 162105.

(14) Gao, M.; Lin, Y.; Bradley, S. T.; Ringel, S. A.; Hwang, J.; Schaff, W. J.; Brillson, L. J. *Appl. Phys. Lett.* **2005**, *87*, 191906.

(15) Wu, Z. H.; Kawai, Y.; Fang, Y.-Y.; Chen, C. Q.; Kondo, H.; Hori, M.; Honda, Y.; Yamaguchi, M.; Amano, H. *Appl. Phys. Lett.* **2011**, *98*, 141905.

(16) Woo, S. Y.; Bugnet, M.; Nguyen, H. P. T.; Mi, Z.; Botton, G. A. *Nano Lett.* **2015**, *15*, 6413−6418.

(17) Ruterana, P.; De Saint Jores, G.; Laügt, M.; Omnes, F.; Bellet-Amalric, E. *Appl. Phys. Lett.* **2001**, *78*, 344−346.

(18) Benamara, M.; Kirste, L.; Albrecht, M.; Benz, K. W.; Strunk, H. *Appl. Phys. Lett.* **2003**, *82*, 547−549.

(19) Laaksonen, K.; Ganchenkova, M.; Nieminen, R. *Phys. B* **2006**, *376−377*, 502−506.

(20) Pavloudis, T.; Kioseoglou, J.; Karakostas, T.; Komninou, P. *Comput. Mater. Sci.* **2016**, *118*, 22−31.

(21) Komsa, H.-P.; Krasheninnikov, A. V. *J. Phys. Chem. Lett.* **2012**, *3*, 3652−3656.

(22) Chen, Y.; Xi, J.; Dumcenco, D. O.; Liu, Z.; Suenaga, K.; Wang, D.; Shuai, Z.; Huang, Y.-S.; Xie, L. *ACS Nano* **2013**, *7*, 4610−4616.

(23) Tongay, S.; Narang, D. S.; Kang, J.; Fan, W.; Ko, C.; Luce, A. V.; Wang, K. X.; Suh, J.; Patel, K. D.; Pathak, V. M.; Li, J.; Wu, J. *Appl. Phys. Lett.* **2014**, *104*, No. 012101.

(24) Siemens, B.; Domke, C.; Ebert, Ph.; Urban, K. *Phys. Rev. B: Condens. Matter Mater. Phys.* **1997**, *56*, 12321−12326.

(25) Steinshnider, J.; Harper, J.; Weimer, M.; Lin, C.-H.; Pei, S. S.; Chow, D. H. *Phys. Rev. Lett.* **2000**, *85*, 4562−4565.

(26) Pfister, M.; Johnson, M. B.; Alvarado, S. F.; Salemink, H. W. M.; Marti, U.; Martin, D.; Morier-Genoud, F.; Reinhart, F. K. *Appl. Phys. Lett.* **1995**, *67*, 1459−1461.

(27) Ebert, Ph.; Heinrich, M.; Simon, M.; Domke, C.; Urban, K.; Shih, C.; Webb, M.; Lagally, M. *Phys. Rev. B: Condens. Matter Mater. Phys.* **1996**, *53*, 4580−4590.

(28) Chao, K.-J.; Shih, C.-K.; Gotthold, D. W.; Streetman, B. G. *Phys. Rev. Lett.* **1997**, *79*, 4822−4825.

(29) McKay, H. A.; Feenstra, R. M.; Schmidtling, T.; Pohl, U. W. *Appl. Phys. Lett.* **2001**, *78*, 82−84.

(30) Hjort, M.; Kratzer, P.; Lehmann, S.; Patel, S. J.; Dick, K. A.; Palmstrøm, C. J.; Timm, R.; Mikkelsen, A. *Nano Lett.* **2017**, *17*, 3634−3640.

(31) Mattias Borg, B.; Wernersson, L.-E. *Nanotechnology* **2013**, *24*, 202001.

(32) The mean force potential equals the pair interaction energy in the low density limit under equilibrium. Hill, T. L. *Statistical Mechanics*; McGraw-Hill, New York, 1956.

(33) Kresse, G.; Furthmüller, J. *Phys. Rev. B: Condens. Matter Mater. Phys.* **1996**, *54*, 11169−11186.

(34) Blöchl, P. E. *Phys. Rev. B: Condens. Matter Mater. Phys.* **1994**, *50*, 17953−17979.

(35) Ceperley, D. M.; Alder, B. J. *Phys. Rev. Lett.* **1980**, *45*, 566−569.

(36) Ebert, Ph.; Zhang, T.; Kluge, F.; Simon, M.; Zhang, Z.; Urban, K. *Phys. Rev. Lett.* **1999**, *83*, 757−760.